

# Multifunctional Linear and Hyperbranched Five-Membered Cyclic Carbonate-Based Polymers Directly Generated from CO<sub>2</sub> and Alkyne-Based Three-Component Polymerization

Bo Song,<sup>†</sup> Tianwen Bai,<sup>§</sup> Xiaotian Xu,<sup>†</sup> Xu Chen,<sup>†</sup> Dongming Liu,<sup>†</sup> Jiali Guo,<sup>†</sup> Anjun Qin,<sup>\*,†,‡</sup> Jun Ling,<sup>\*,§,‡</sup> and Ben Zhong Tang<sup>\*,†,‡,§</sup>

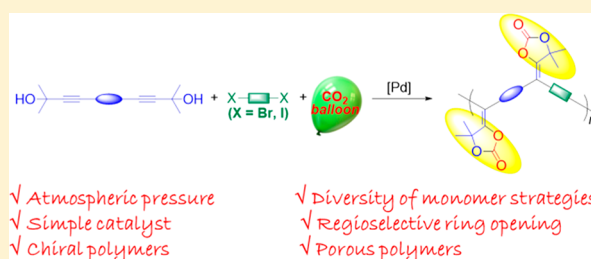
<sup>†</sup>State Key Laboratory of Luminescent Materials and Devices, Center for Aggregation-Induced Emission, South China University of Technology, Guangzhou 510640, China

<sup>‡</sup>Department of Chemistry, Hong Kong Branch of Chinese National Engineering Research Center for Tissue Restoration and Reconstruction, Institute for Advanced Study, and Department of Chemical and Biological Engineering, The Hong Kong University of Science & Technology, Clear Water Bay, Kowloon, Hong Kong, China

<sup>§</sup>MOE Key Laboratory of Macromolecular Synthesis and Functionalization, Department of Polymer Science and Engineering, Zhejiang University, Hangzhou 310027, China

## Supporting Information

**ABSTRACT:** Fixing carbon dioxide (CO<sub>2</sub>) into polymeric materials is a subject of enduring interest but limited to very few efficient polymerizations. In this work, a facile Pd(OAc)<sub>2</sub>/LiO<sup>t</sup>Bu-catalyzed one-pot, three-component polymerization of CO<sub>2</sub>, bis(propargylic alcohol)s, and aryl dihalides under atmospheric pressure is developed. Linear and hyperbranched multifunctional five-membered cyclic carbonate (SCC)-based polymers with well-defined structures, high weight-average molecular weights (*M<sub>w</sub>* up to 42500), and versatile properties such as aggregation-induced emission as well as chiral and porous properties are successfully produced in excellent yields (up to 96%). The reaction mechanism was well investigated via the density functional theory calculation and *in situ* Fourier transform infrared spectroscopy, both indicating that there is synergistic reaction effect among CO<sub>2</sub>, bis(propargylic alcohol)s, and aryl dihalides. The polymers could be postfunctionalized by amines via catalyst-free regioselective ring-opening reaction with 100% grafting ratio. Thus, this work not only develops a new way to directly fix CO<sub>2</sub> into polymeric materials but also provides the SCC-based polymers with versatile properties, showing great potentials in diverse areas.



## INTRODUCTION

Using carbon dioxide (CO<sub>2</sub>) as a feedstock to generate thousands of compounds has drawn much attention.<sup>1,2</sup> Today, it is also highly desirable to use CO<sub>2</sub> to prepare polymeric materials because of their widespread needs. In general, there are two ways to obtain polymeric materials from CO<sub>2</sub>. One is converting CO<sub>2</sub> into monomers for further polymerization, such as ethylene,<sup>3</sup> furan-2,5-dicarboxylic acid,<sup>4</sup> and bis(five-membered cyclic carbonates) (SCC).<sup>5,6</sup> In particular, lactone intermediates synthesized from CO<sub>2</sub> have recently emerged as a new class of monomers for polymerization.<sup>7–10</sup> The other is directly using CO<sub>2</sub> as a monomer to generate polymers.<sup>11–27</sup> They are both significant for the synthesis of CO<sub>2</sub>-based polymeric materials.

As a vital monomer for polymerization, CO<sub>2</sub> has been studied for many years. The polymers like poly(urethane)s, polyureas, and polycarbonates can be obtained directly from CO<sub>2</sub>.<sup>11,12</sup> Among these polymers, poly(propylene carbonate)s, generated from the CO<sub>2</sub>/propylene oxide copolymerization, are the most well-known and widely studied one.<sup>13–27</sup> This is

an efficient way to synthesize phosgene-free polycarbonates, which has been industrialized.<sup>28</sup> However, CO<sub>2</sub>-based functional polymers were rarely reported compared to general polymers.<sup>29</sup> Thus, exploring new efficient polymerizations of CO<sub>2</sub> under mild reaction conditions and atmosphere pressure to generate CO<sub>2</sub>-based functional polymers is highly desirable.

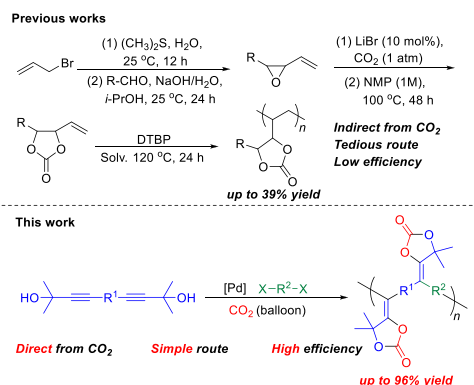
The SCC-based polymers are a new kind of CO<sub>2</sub>-based functional ones.<sup>30,31</sup> They not only possess various properties but also can act as a versatile platform toward functional polymers.<sup>32–34</sup> For example, Endo et al. reported an indirect way to obtain SCC-based polymers from CO<sub>2</sub>.<sup>35–37</sup> First, they synthesized a monomeric SCC with the vinyl group from CO<sub>2</sub> via several steps. Then they used this monomer for further radical polymerization (Scheme 1). The obtained polymers can undergo color change with acid–base switching for sensing applications. It is a new way to obtain functional SCC-based

Received: May 2, 2019

Revised: June 27, 2019

Published: July 17, 2019

### Scheme 1. Synthetic Routes of SCC-Based Polymers under Atmospheric Pressure



polymers from CO<sub>2</sub>, but the synthetic routes are tedious. Thus, we would like to explore a new, simple, and efficient way to generate functional SCC-based polymers directly from CO<sub>2</sub>.

We found that SCC obtained from CO<sub>2</sub> and propargylic alcohols still has carbon–carbon double bonds, which might react further with other compounds. So we put forward the hypothesis that introducing a third monomer to react with CO<sub>2</sub> and bis(propargylic alcohol)s might generate SCC-based polymers. After searching for plenty of organic reactions, aryl halides came to our attention.<sup>38–40</sup> For example, Cheng et al. reported an elegant CO<sub>2</sub>-based three-component reaction, in which aryl halides could couple with carbon–carbon double bonds in the presence of palladium catalyst without damaging the structure of SCC.<sup>40</sup> Thus, one-step conversion of CO<sub>2</sub> to SCC-based polymers might be realized.

Following this idea, in this work, a new one-pot, three-component polymerization of CO<sub>2</sub>, bis(propargylic alcohol)s, and aryl dihalides was successfully developed. This polymerization could be facily performed in the presence of Pd(OAc)<sub>2</sub>/LiO<sup>t</sup>Bu catalytic system in *N,N*-dimethylformamide (DMF) under atmospheric pressure. Soluble and thermally stable SCC-based polymers with high molecular weights were obtained in high yields after a few hours (Schemes 1 and 2). Furthermore, an “AB” type monomer could also be easily synthesized and polymerized to generate functional SCC-based

polymer. The polymerization mechanism was studied via *in situ* Fourier transform infrared spectroscopy (FT-IR) and density functional theory (DFT) calculation, both indicating that there exists synergistic reaction effect among CO<sub>2</sub>, bis(propargylic alcohol)s, and aryl dihalides. What is more, the resultant polymers could be postfunctionalized by amines via catalyst-free regioselective ring-opening reaction with unity grafting ratio. Moreover, tetraphenylethene (TPE) and binaphthyl units could be facily incorporated into polymers to endow the resultant polymers with aggregation-induced emission (AIE) and chiral properties, respectively. Because of the flexibility for the design of monomers, hyperbranched SCC-based polymers could also be generated via versatile monomer combinations and porous polymers with BET surface area as high as 172 m<sup>2</sup>/g could be constructed.

## RESULTS AND DISCUSSION

**Polymerization.** All the bis(propargylic alcohol) monomers **1a–1d** were prepared via Sonogashira coupling reaction (Scheme S1). All the aryl dihalide monomers **2a–2e** are commercially available or could be prepared with ease. All monomers used in this work are stable under ambient conditions. To obtain polymers with high weight-average molecular weight (*M<sub>w</sub>*) values in high yields, **1a** and **2a** were used as representative monomers to polymerize with CO<sub>2</sub> (balloon) to investigate the reaction conditions, such as the catalysts and their loading ratio, reaction time, solvent, monomer concentration, reaction temperature, and the base. The results showed that the polymerization could be well performed in DMF with a monomer concentration of 0.1 M at 80 °C for 4 h in the presence of 10 mol % Pd(OAc)<sub>2</sub> catalyst under normal pressure (Tables S1–S7).

Next, we polymerized various types of monomers with CO<sub>2</sub> under the optimal conditions to test the robustness and universality of this polymerization (Table 1). To our surprise, some monomers showed much higher reactivity, so the SCC-based polymers could be generated in a shorter time. For example, **11b/2b/CO<sub>2</sub>** with a *M<sub>w</sub>* of 42500 could be obtained in 96% yield in only 30 min. We believe that polymers with higher molecular weights could be generated upon changing the reaction conditions. In addition, aryl dibromides also showed high reactivity, greatly expanding the scope of the

Scheme 2. Polymerization of Carbon Dioxide, **1**, and **2**

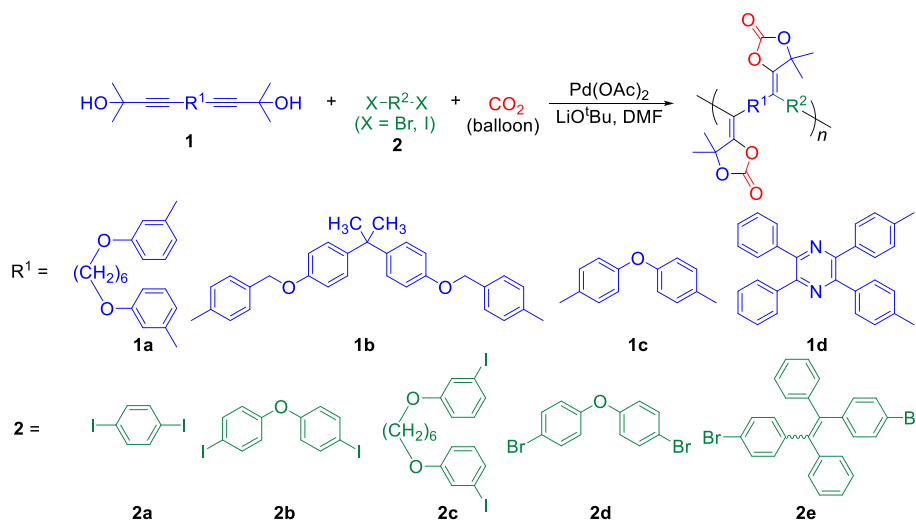


Table 1. Polymerization Results of Different Monomers<sup>a</sup>

| entry          | polymer                | yield (%) | $M_w^b$ | $\bar{D}^b$ |
|----------------|------------------------|-----------|---------|-------------|
| 1              | P1a/2a/CO <sub>2</sub> | 92        | 16000   | 1.82        |
| 2              | P1b/2a/CO <sub>2</sub> | 88        | 19700   | 2.22        |
| 3 <sup>c</sup> | P1c/2a/CO <sub>2</sub> | 85        | 12900   | 1.67        |
| 4              | P1d/2a/CO <sub>2</sub> | 84        | 10800   | 1.60        |
| 5 <sup>c</sup> | P1a/2b/CO <sub>2</sub> | 91        | 30000   | 2.20        |
| 6 <sup>d</sup> | P1b/2b/CO <sub>2</sub> | 96        | 42500   | 2.81        |
| 7 <sup>e</sup> | P1b/2c/CO <sub>2</sub> | 83        | 13700   | 1.71        |
| 8              | P1b/2d/CO <sub>2</sub> | 77        | 13400   | 2.11        |
| 9 <sup>f</sup> | P1a/2e/CO <sub>2</sub> | 90        | 33200   | 2.29        |

<sup>a</sup>Carried out in DMF at 80 °C for 4 h in the presence of Pd(OAc)<sub>2</sub> and LiO<sup>t</sup>Bu under normal pressure. [1a] = [2a] = 0.10 M, [1a]/[2a]/[Pd(OAc)<sub>2</sub>]/[LiO<sup>t</sup>Bu] = 1:1:0.1:6. <sup>b</sup>Polydispersity index ( $\bar{D}$ ) and weight-average molecular weight ( $M_w$ ) were estimated by advanced polymer chromatography (APC) using THF as an eluent on the basis of a polystyrene calibration. <sup>c</sup>Reaction time ( $t$ ) = 2.5 h. <sup>d</sup> $t$  = 0.5 h. <sup>e</sup> $t$  = 3 h. <sup>f</sup> $t$  = 2 h.

monomers. What is more, the polymerization of AB type monomer with CO<sub>2</sub> could also produce a soluble cross-conjugated polymer with a  $M_w$  value of 29100 in 84% yield (Scheme 3). This monomer strategy could greatly simplify experimental operation.

All the resultant polymers showed good solubility in commonly used organic solvents. The thermogravimetric analysis (TGA) and differential scanning calorimeter (DSC) results indicated that the 5% weight loss temperatures ( $T_d$ ) and the glass-transition temperatures ( $T_g$ ) of the polymers are in the ranges 210–268 °C (Figure S1) and 95–135 °C (Figure S2), respectively, suggesting that they are thermally stable.

**Structural Characterization.** The structures of polymers were characterized by FT-IR, <sup>1</sup>H NMR, and <sup>13</sup>C NMR spectra, and satisfactory analytical data corresponding to their structures were obtained. Herein, we took P1a/2a/CO<sub>2</sub> as an example for structural analysis. To help us to confirm the structure of polymer, model compound 4 was synthesized from 1a, iodobenzene, and CO<sub>2</sub> under the same reaction conditions (Scheme S2). In the FT-IR spectra (Figure 1), the O–H stretching vibration of 1a was observed at 3330 cm<sup>−1</sup>. In both the spectra of 4 and P1a/2a/CO<sub>2</sub>, O–H stretching vibration peaks disappeared. Meanwhile, a new peak associated with C=O stretching vibration appeared at 1819 cm<sup>−1</sup>, confirming the occurrence of this polymerization. Similar results were obtained in the FT-IR spectra of other polymers (Figures S3–S9).

Their <sup>1</sup>H NMR spectra of P1a/2a/CO<sub>2</sub> and its monomers and model compound are also compared in Figure 2. The –OH protons and –CH<sub>3</sub> protons of 1a were resonated at  $\delta$  2.10 (d) and 1.58 (a), respectively. In the spectra of 4 and P1a/2a/CO<sub>2</sub>, the –OH proton resonance disappeared and the –CH<sub>3</sub> proton resonant peak was shifted to  $\delta$  1.44 (g). In

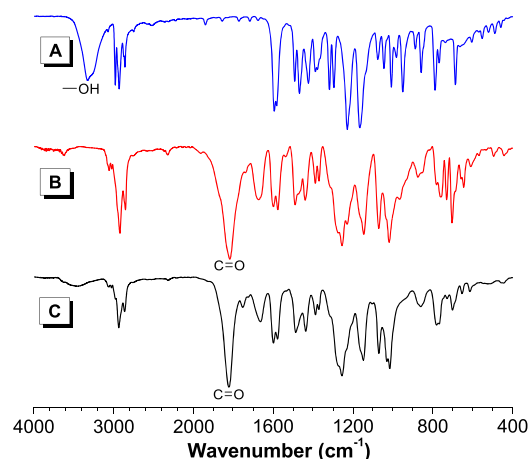


Figure 1. FT-IR spectra of (A) monomer 1a, (B) model compound 4, and (C) polymer P1a/2a/CO<sub>2</sub>.

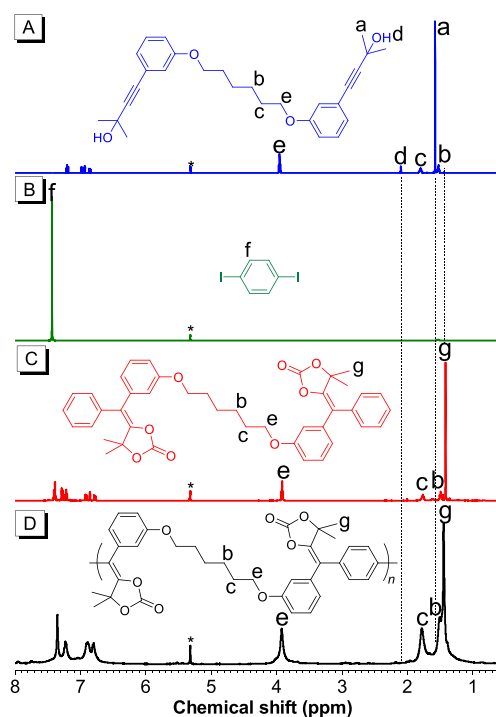
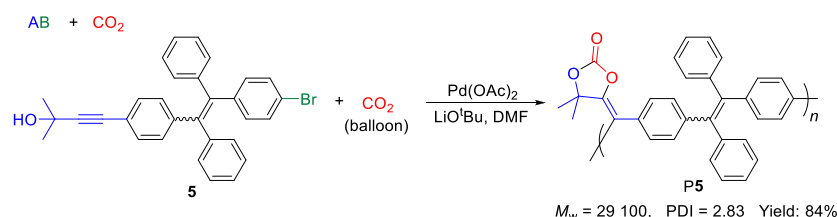
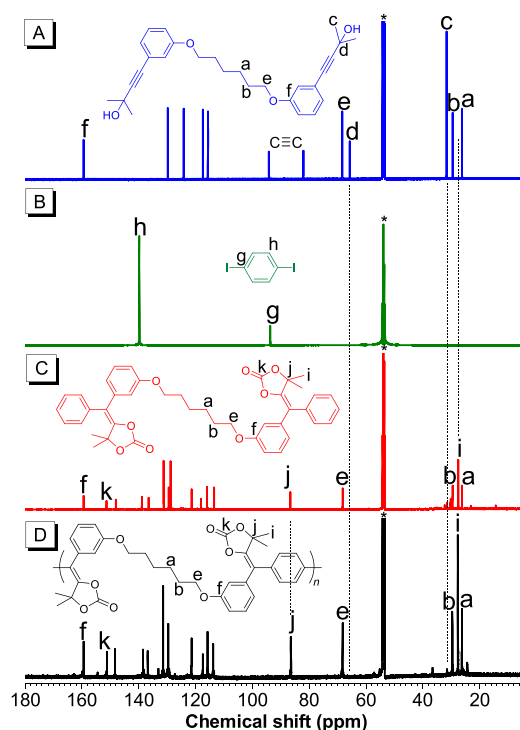


Figure 2. <sup>1</sup>H NMR spectra of (A) monomer 1a, (B) monomer 2a, (C) model compound 4, and (D) polymer P1a/2a/CO<sub>2</sub> in DCM-*d*<sub>2</sub>. The solvent peaks are marked with asterisks.

addition, <sup>13</sup>C NMR spectroscopy could provide more detailed structural information. As shown in Figure 3, the ethynyl carbons of 1a were resonated at  $\delta$  94.16 and 82.11, which could not be found in the spectra of 4 and P1a/2a/CO<sub>2</sub>. The –CH<sub>3</sub> carbons and quaternary carbons adjacent to ethynyl

### Scheme 3. Synthesis of SCC-Based Polymers via the “AB + CO<sub>2</sub>” Monomer Strategy





**Figure 3.**  $^{13}\text{C}$  NMR spectra of (A) monomer **1a**, (B) monomer **2a**, (C) model compound **4**, and (D) polymer **P1a/2a/CO<sub>2</sub>** in  $\text{DCM-d}_2$ . The solvent peaks are marked with asterisks.

groups of **1a** resonate at  $\delta$  31.71 (c), and 65.80 (d), respectively, which were shifted to  $\delta$  27.67 (i) and 86.43 (j) in the spectra of **4** and **P1a/2a/CO<sub>2</sub>** due to the different chemical environment of carbons in propargylic alcohol and SCC. Furthermore, a new peak associated with the resonances of carbonate carbons appeared at  $\delta$  151.17 in **4** and **P1a/2a/CO<sub>2</sub>**. All the  $^1\text{H}$  and  $^{13}\text{C}$  NMR spectra confirmed the structures of **P1a/2a/CO<sub>2</sub>**. It is worth noting that the  $^1\text{H}$  and  $^{13}\text{C}$  NMR spectral data of other polymers are summarized in the Supporting Information and all solidly confirmed their respective structures (Figures S10–S25).

**Mechanism Investigation.** To deeply understand the reaction mechanism, we performed a theoretical calculation. We used **AH** and iodobenzene as model compounds to simplify the calculation and employed the powerful DFT to analyze the whole process of the reaction. The proposed routes are shown in Scheme 4 and Figure 4 with selected 3D geometries and coordinates in the Supporting Information.

First, the lithium carbonate **A** is produced by addition of  $\text{CO}_2$  on lithium alkoxide **AL**, and  $\text{Pd(II)}$  inserts into C–I bond of iodobenzene to form compound **B**. Second, **A** is coordinated with **B** and acetate ligands to form **C<sub>0</sub>**. After leaving acetate ligands, the stable intermediate complex **C<sub>1</sub>** is obtained. Third, the oxygen atom on carbonate attacks the ethynyl group catalyzed by  $\text{Pd(II)}$  of the  $\text{sp}^3$  state in complex **CD<sub>TS</sub>** to produce the cyclic carbonate structure **C<sub>2</sub>**. The phenyl and iodine ligand rotate to exchange their position to form **C<sub>3</sub>** and released equivalent  $\text{LiI}$  to generate **D**. Finally,  $\text{Pd(0)}$  forms by the reductive elimination of vinyl and aryl groups from  $\text{Pd(II)}$ . Thus, product **E** is obtained (Scheme 4).

In the total reaction, the insertion of  $\text{Pd(II)}$  with Gibbs free energy barrier of  $\Delta G_{\text{B}} = 28.66$  kcal/mol could be easily overcome at 80 °C. The coordination of **A**, **B**, and acetate

ligands is feasible due to the formation of semipolar bonds between  $\text{Pd(II)}$  and  $\text{C}\equiv\text{C}$  as well as  $\text{Li}^+$  and a phenyl group. The Gibbs free energy barrier between **C<sub>1</sub>** and **C<sub>2</sub>** is confirmed as  $\Delta G_{\text{CD}} = 20.51$  kcal/mol, and the Gibbs free energy of **C<sub>2</sub>** is quite lower than that of **C<sub>1</sub>**, indicating that the cyclization reaction is quite efficient. Moreover, the  $\text{Pd(0)}$  is released from **D** with  $\Delta G_{\text{DE}} = 15.41$  kcal/mol, and final product **E** shows extremely low Gibbs free energy, so it is a swift transformation from **D** to **E**.

According to theoretical mechanism research, the polymerization we developed could propagate efficiently under mild conditions. Moreover, there might be synergistic reaction effect among  $\text{CO}_2$ , aryl dihalides, and bis(propargylic alcohol)s. The aryl dihalides play a vital role in the cyclization to form the cyclic carbonates during this polymerization.

To verify the results of theoretical calculation, we first used **1c** to react with  $\text{CO}_2$  under the optimized reaction conditions without addition of **2a**. However, we cannot get the bis(SCC) intermediates (Scheme S3), suggesting that the SCC cannot be formed without aryl dihalides. Then we designed a three-step reaction of **1c**, **2a**, and  $\text{CO}_2$ , which was monitored by the *in situ* FT-IR spectrometry (Figure 5A). In the first step, the monomer **1c** was placed under  $\text{CO}_2$  atmosphere (balloon) in the presence of  $\text{LiO}^t\text{Bu}$  in DMF. From Figure 5, we could find that a new peak associated with the carbonate groups at  $1820\text{ cm}^{-1}$  emerged and soon became balanced. According to the DFT results, the reason was that the lithium carbonate intermediate was produced from **1c**,  $\text{CO}_2$ , and  $\text{LiO}^t\text{Bu}$ , and there is a reaction balance between **1c** and the lithium carbonate intermediate because of a very small Gibbs free energy barrier between them. In the second step, the catalyst of  $\text{Pd(OAc)}_2$  was added, but almost no change was observed in the kinetic and 3D FT-IR profiles (Figure 5B,C). Because  $\text{Pd(OAc)}_2$  itself could not catalyze the cyclization of the lithium carbonate intermediate, thus, the reaction balance remained unchanged. In the third step, when monomer **2a** was added, the peak at  $1820\text{ cm}^{-1}$  increased fast and became balanced again in 1 h. The reason might be that  $\text{Pd(II)}$  species could insert into the C–I bond of **2a**, further facilitating the cyclization of the lithium carbonate intermediate and promoting the balance forward running. Thus, our experimental results agree well with the theoretical calculation and the proposed mechanism by Cheng et al.<sup>40</sup>

**Regioselective Ring-Opening Reaction.** The SCC could react with nucleophiles via the ring-opening reaction as reported previously;<sup>5,6</sup> we thus postfunctionalized **P1a/2a/CO<sub>2</sub>** by using the nucleophile of diethylamine in DMF at 50 °C without addition of any catalyst, and the urethane-based polymer **P6** was readily yielded (Scheme 5). Theoretically, two regioisomers could be formed, but we just got one, indicating that the ring-opening reaction is regioselective. The structure of resultant polymer was characterized by  $^1\text{H}$  and  $^{13}\text{C}$  NMR spectra. As shown in the  $^1\text{H}$  NMR spectrum (Figure S26), the proton of chiral carbon adjacent to the carbonyl group emerged at  $\delta$  5.40. Meanwhile, the protons of a methylene group adjacent to the urethane group resonated at  $\delta$  3.40–3.11. The  $^{13}\text{C}$  NMR spectrum can provide more information about the structures (Figure S27). The carbonyl carbon, urethane carbon, and chiral carbon adjacent to the carbonyl group resonate at  $\delta$  207.87, 154.82, and 56.96, respectively, further confirming the structures of regioregular urethane-based polymers.

Scheme 4. Proposed Mechanism of Polymerization

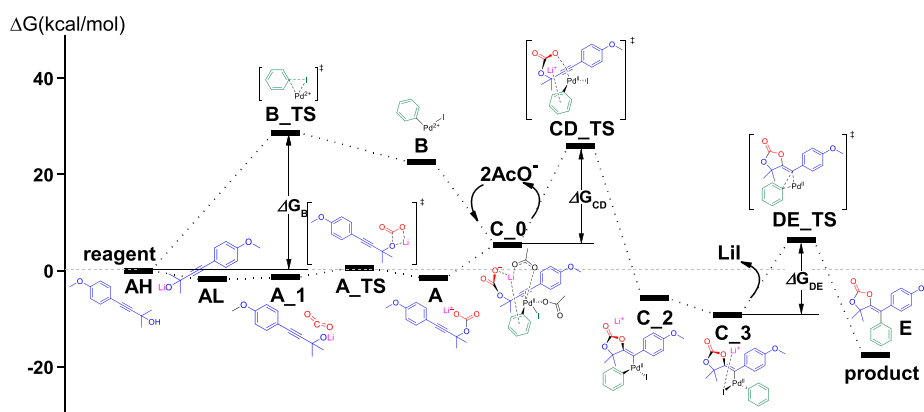
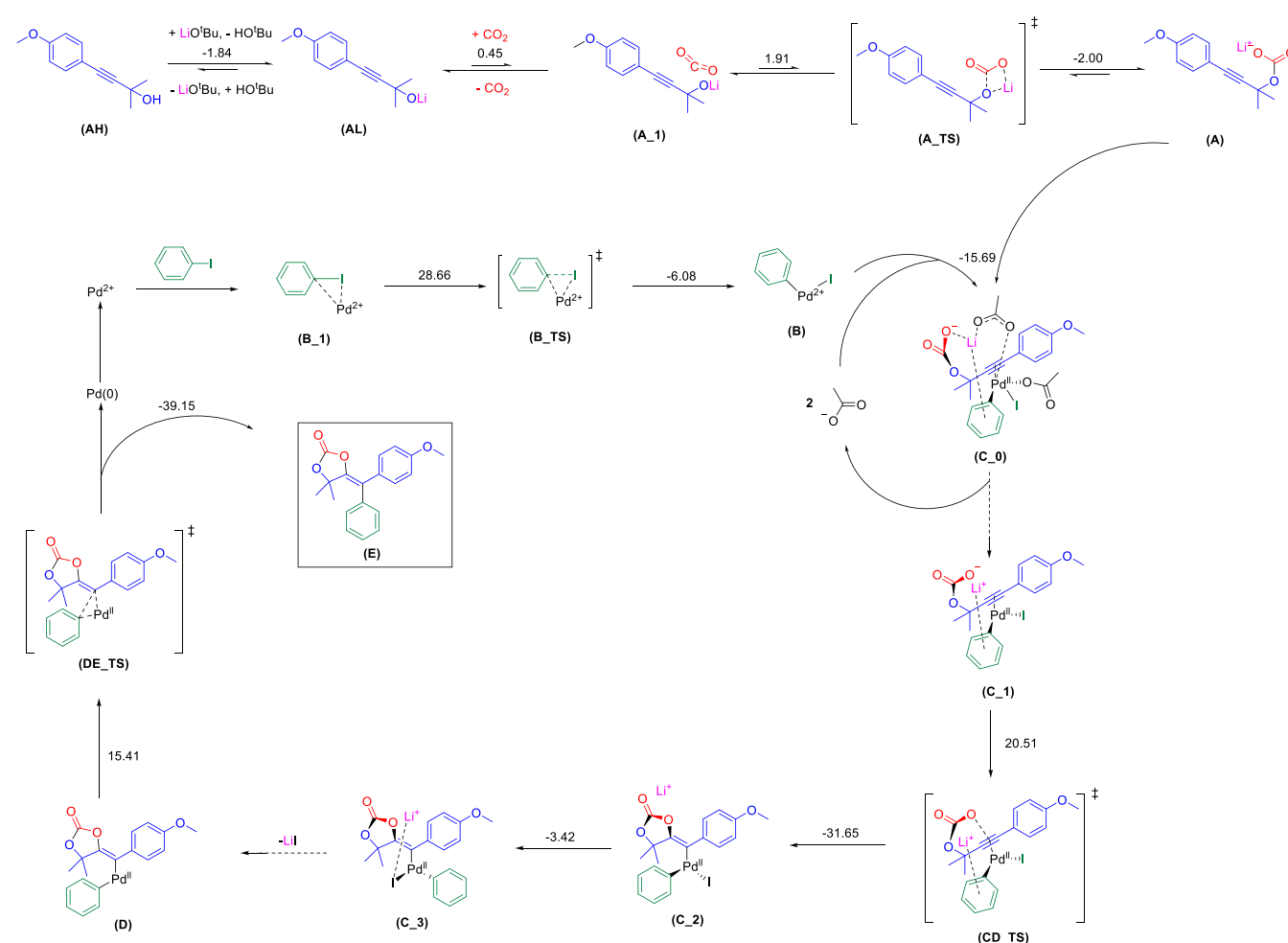


**Figure 4.** DFT calculated profiles of the whole process shown in Scheme 4. The Gibbs free energy (in kcal/mol) barriers are  $\Delta G_B = 28.66$ ,  $\Delta G_{CD} = 20.51$ , and  $\Delta G_{DE} = 15.41$ .

We also employed the DFT to follow the whole process of the ring-opening reaction (Scheme S4 and Figure S28). The selectivity of the ring-opening step was confirmed with a  $\Delta\Delta G = 9.00$  kcal/mol, which indicated that the ring-opening reaction of diphenylethyl side was preferred.

**AIE and Chiral Properties.** Thanks to the functional group tolerance of our developed polymerization, the AIE-active TPE unit could be readily introduced into the polymer skeletons of P5 and P1a/2e/CO<sub>2</sub>.<sup>41</sup> We measured their

photoluminescence (PL) spectra in THF and THF/water mixtures with different water fraction ( $f_w$ ) (Figure 6, Figure S29, and Table S8). They emit faintly in THF, but their emission intensity increased with addition of poor solvent of water. Both P5 and P1a/2e/CO<sub>2</sub> showed the highest fluorescence intensity at the  $f_w$  of 90%, which are 22 and 9 times higher than that of their THF solutions, respectively. These results further confirmed their AIE feature.

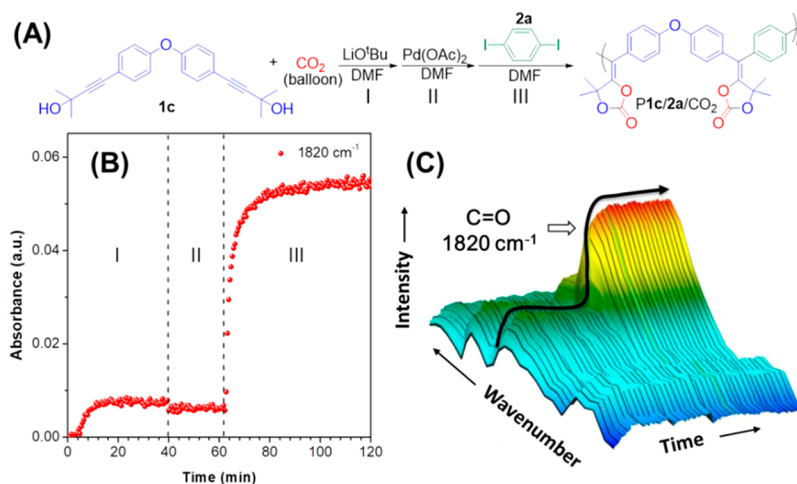


Figure 5. (A)  $\text{CO}_2$  and alkyne-base three-step reaction, (B) kinetic profiles, and (C) 3D FT-IR profile of the reaction.

#### Scheme 5. Regioselective Ring-Opening of P1a/2a/ $\text{CO}_2$

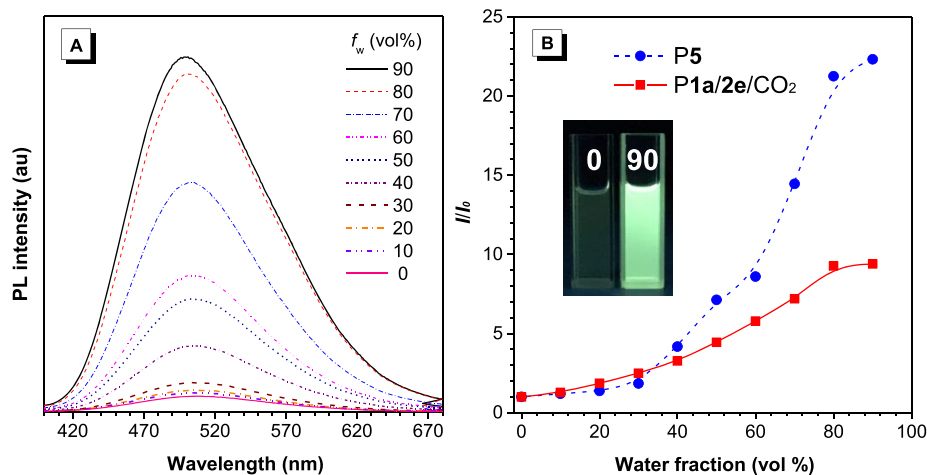
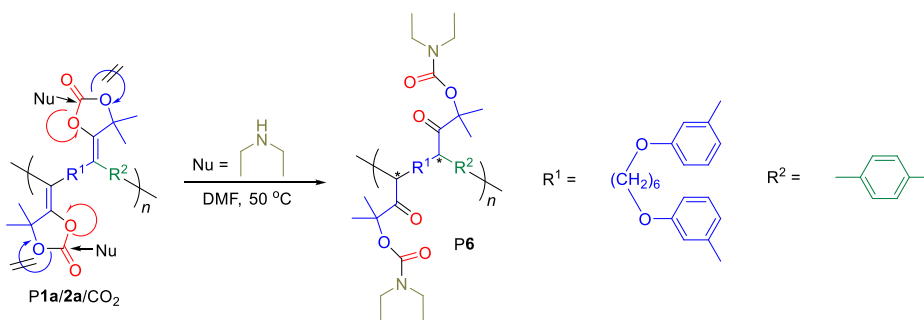
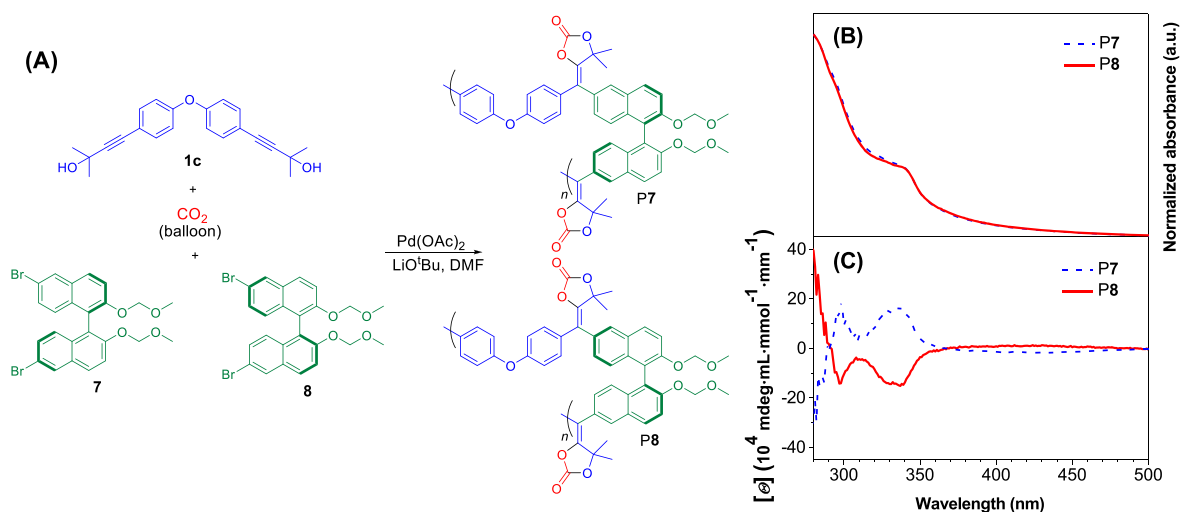


Figure 6. (A) PL spectra of **P5** in THF and THF/water mixtures. Concentration:  $10\text{ }\mu\text{M}$ .  $\lambda_{\text{ex}}$ :  $330\text{ nm}$ . (B) Plot of relative PL intensity versus water fraction in THF/water mixtures, where  $I$  = peak intensity in water mixtures and  $I_0$  = peak intensity in pure THF. Inset in panel B: photographs of **P5** in pure THF and a THF/water mixture with 90% water.

In addition, optically active monomers **7** and **8** could be used to polymerize with  $\text{CO}_2$  and **1c** and to synthesize chiral polymers **P7** and **P8** (Figure 7A).<sup>42</sup> Through  $^1\text{H}$  and  $^{13}\text{C}$  NMR spectral analysis (Figures S30–S33), the structures of **P7** and **P8** were confirmed. Then the UV and circular dichroism (CD) spectra of the polymers were measured, and the data are summarized in Figure 7B,C. The results showed that they exhibited similar UV spectral profiles. However, their CD spectra are quite different, showing symmetrical property with

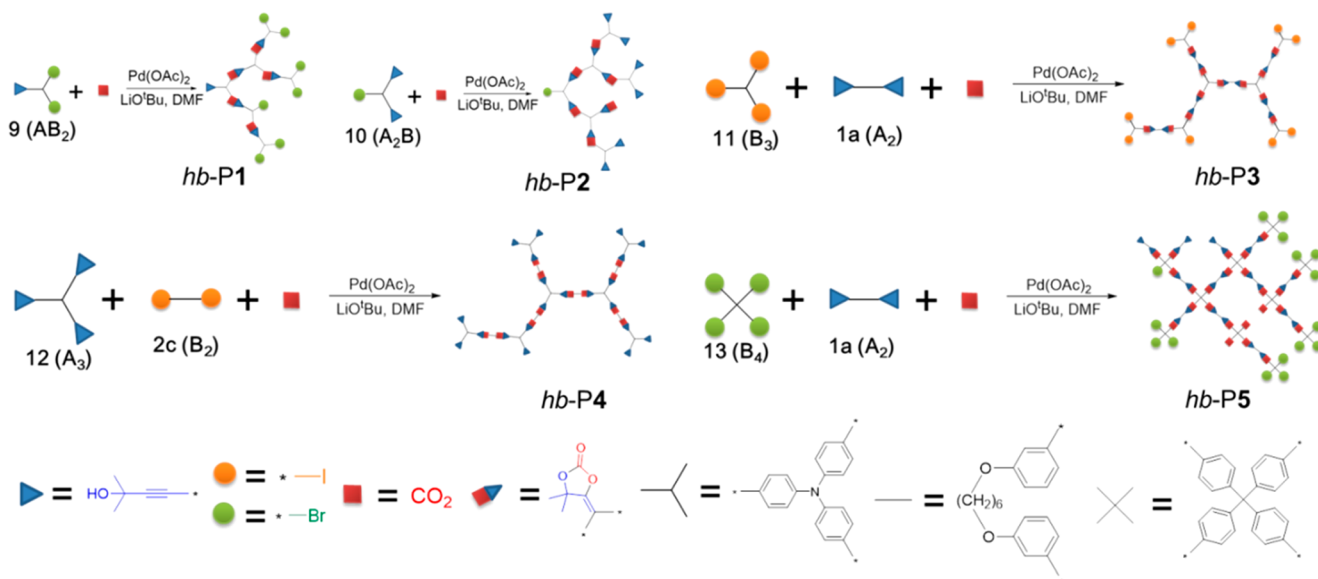
two same peaks centered at  $298$  and  $338\text{ nm}$ . The CD results demonstrate that **P7** and **P8** also retain chiral properties.

**Hyperbranched and Porous Polymers.** Hyperbranched polymers are a new class of macromolecules, which exhibit unique architectures and properties.<sup>43–45</sup> Developing hyperbranched polymers based on  $\text{CO}_2$  is quite significant because it can not only increase  $\text{CO}_2$  incorporation ratio in polymers but also bring multifunctional properties to them. Thanks to the flexibility for the design of multifunctionalized monomers, diverse monomer combinations were used to construct



**Figure 7.** (A) Syntheses of chiral polymers. (B) UV and (C) CD spectra of P7 and P8 in THF solutions (solution concentration: 10<sup>−4</sup> M).

### Scheme 6. Syntheses of Hyperbranched Polymers via Diverse Monomer Combinations



hyperbranched polymers with different architectures. Aryl trihalide **14** was used to synthesize monomers of AB<sub>2</sub> (**9**), A<sub>2</sub>B (**10**), and A<sub>3</sub> (**12**) types via one-pot Sonogashira coupling reaction as shown in Scheme S5. First, monomer **9** was employed to react with CO<sub>2</sub> in the presence of Pd(OAc)<sub>2</sub>/LiO<sup>t</sup>Bu in DMF and hyperbranched polymers were readily yielded (Scheme 6). For example, *hb*-P1 with high *M<sub>w</sub>* (12100) could be obtained by this efficient polymerization. According to <sup>1</sup>H and <sup>13</sup>C NMR spectra of *hb*-P1 (Figures S34 and S35), almost all resonant peaks associated with propargylic alcohols could not be observed, indicative of nearly 100% monomer conversion. Similarly, *hb*-P2 could be generated from the polymerization of monomer **10** and CO<sub>2</sub> (Scheme 5). The difference of *hb*-P2 from *hb*-P1 is that obvious resonance peaks of propargylic alcohols could be found in the <sup>1</sup>H and <sup>13</sup>C NMR spectra (Figures S34 and S35) because the number of propargylic alcohol groups is twice as many as bromide groups; there are still many unreacted propargylic alcohols on the periphery of *hb*-P2. It is worth noting that other different monomer strategies like “B<sub>3</sub> + A<sub>2</sub> + CO<sub>2</sub>”, “A<sub>3</sub> + B<sub>2</sub> + CO<sub>2</sub>”, and “B<sub>4</sub> + A<sub>2</sub> + CO<sub>2</sub>” could also be used to construct

hyperbranched polymers with high *M<sub>w</sub>* values (up to 26700) (Scheme 6).

Moreover, the “B<sub>4</sub> + A<sub>2</sub> + CO<sub>2</sub>” monomer strategy was used to synthesize insoluble porous polymers of *hb*-P6 (Scheme S6). In the FT-IR spectrum of *hb*-P6, C=O stretching vibrations could be observed at 1819 cm<sup>−1</sup>, suggestive of the formation of cyclic carbonates in *hb*-P6 (Figure S36). Thanks to its porous feature, the Brunauer–Emmett–Teller (BET) surface area of *hb*-P6 was measured to be 172 m<sup>2</sup> g<sup>−1</sup> (Figure S37), showing great potential as gas adsorbent materials.

### CONCLUSIONS

In this work, we developed a powerful one-pot, three-component polymerization of CO<sub>2</sub>, bis(propargylic alcohol)s, and aryl dihalides toward the SCC-based polymers. This polymerization enjoys such unique advantages as mild reaction conditions under atmospheric pressure, a simple and commercially available catalytic system, and versatile monomer combinations. The *in situ* FT-IR and DFT calculation unveiled the reaction mechanism, which suggests that this polymer-

ization is highly efficient under mild reaction conditions and there exists a synergistic reaction effect among CO<sub>2</sub>, bis-(propargylic alcohol)s, and aryl dihalides. Moreover, the SCC-based polymers could be postfunctionalized by amines via catalyst-free regioselective ring-opening reaction with unity grafting ratio. Thanks to its excellent functional group tolerance, the TPE and binaphthyl units could be facilely incorporated into the polymers to endow them with unique AIE and chiral properties, respectively. Hyperbranched polymers could also be generated from CO<sub>2</sub> via versatile monomer combinations in high conversion rates, and the porous polymers with BET surface area as high as 172 m<sup>2</sup>/g could be constructed. Thus, this work not only establishes a new CO<sub>2</sub>-based polymerization but also furnishes the SCC-based polymers with excellent and versatile properties, showing great potential in diverse areas.

## ■ ASSOCIATED CONTENT

### Supporting Information

The Supporting Information is available free of charge on the ACS Publications website at DOI: 10.1021/acs.macromol.9b00898.

Experimental details, reaction condition optimization parameters, characterization data (TGA, DSC, FT-IR, NMR, UV, PL, etc.), 3-D geometries, and coordinates of the calculated model compounds (PDF)

## ■ AUTHOR INFORMATION

### Corresponding Authors

\*E-mail [msqinaj@scut.edu.cn](mailto:msqinaj@scut.edu.cn) (A.J.Q.).

\*E-mail [lingjun@zju.edu.cn](mailto:lingjun@zju.edu.cn) (L.J.).

\*E-mail [tangbenz@ust.hk](mailto:tangbenz@ust.hk) (B.Z.T.).

### ORCID

Anjun Qin: 0000-0001-7158-1808

Jun Ling: 0000-0002-0365-1381

Ben Zhong Tang: 0000-0002-0293-964X

### Author Contributions

B.S. and T.B. contributed equally to this work.

### Notes

The authors declare no competing financial interest.

## ■ ACKNOWLEDGMENTS

This work was financially supported by the National Natural Science Foundation of China (21788102, 21525417, and 21490571), the Natural Science Foundation of Guangdong Province (2016A030312002 and 2019B030301003), the Fundamental Research Funds for the Central Universities (2015ZY013), and the Innovation and Technology Commission of Hong Kong (ITC-CNERC14S01).

## ■ REFERENCES

- (1) Aresta, M.; Dibenedetto, A.; Angelini, A. Catalysis for The Valorization of Exhaust Carbon: from CO<sub>2</sub> to Chemicals, Materials, and Fuels. Technological Use of CO<sub>2</sub>. *Chem. Rev.* **2014**, *114*, 1709–1742.
- (2) Mikkelsen, M.; Jørgensen, M.; Krebs, F. C. The Teraton Challenge. A Review of Fixation and Transformation of Carbon Dioxide. *Energy Environ. Sci.* **2010**, *3*, 43–81.
- (3) De Luna, P.; Quintero-Bermudez, R.; Dinh, C.-T.; Ross, M. B.; Bushuyev, O. S.; Todorović, P.; Regier, T.; Kelley, S. O.; Yang, P.; Sargent, E. H. Catalyst Electro-redeposition Controls Morphology

and Oxidation State for Selective Carbon Dioxide Reduction. *Nat. Catal.* **2018**, *1*, 103–110.

- (4) Banerjee, A.; Dick, G. R.; Yoshino, T.; Kanan, M. W. Carbon Dioxide Utilization via Carbonate-promoted C-H Carboxylation. *Nature* **2016**, *531*, 215–219.

- (5) Maisonneuve, L.; Lamarzelle, O.; Rix, E.; Grau, E.; Cramail, H. Isocyanate-Free Routes to Polyurethanes and Poly(hydroxyl Urethane)s. *Chem. Rev.* **2015**, *115*, 12407–12439.

- (6) Gennen, S.; Grignard, B.; Tassaing, T.; Jerome, C.; Detrembleur, C. CO<sub>2</sub>-Sourced  $\alpha$ -Alkylidene Cyclic Carbonates: A Step Forward in the Quest for Functional Regioregular Poly(urethane)s and Poly(carbonate)s. *Angew. Chem., Int. Ed.* **2017**, *56*, 10394–10398.

- (7) Nakano, R.; Ito, S.; Nozaki, K. Copolymerization of Carbon Dioxide and Butadiene via  $\alpha$ -Lactone Intermediate. *Nat. Chem.* **2014**, *6*, 325–331.

- (8) Xu, Y. C.; Zhou, H.; Sun, X. Y.; Ren, W. M.; Lu, X. B. Crystalline Polyesters from CO<sub>2</sub> and 2-Butyne via  $\alpha$ -Methylene- $\beta$ -Butyrolactone Intermediate. *Macromolecules* **2016**, *49*, 5782–5787.

- (9) Liu, M.; Sun, Y.; Liang, Y.; Lin, B. L. Highly Efficient Synthesis of Functionalizable Polymers from CO<sub>2</sub>/1,3-Butadiene-Derived Lactone. *ACS Macro Lett.* **2017**, *6*, 1373–1378.

- (10) Zhang, Y.; Xia, J.; Song, J.; Zhang, J.; Ni, X.; Jian, Z. Combination of Ethylene, 1,3-Butadiene, and Carbon Dioxide into Ester-Functionalized Polyethylenes via Palladium-Catalyzed Coupling and Insertion Polymerization. *Macromolecules* **2019**, *52*, 2504–2512.

- (11) Chen, Z.; Hadjichristidis, N.; Feng, X.; Gnanou, Y. Poly(urethane-carbonate)s from Carbon Dioxide. *Macromolecules* **2017**, *50*, 2320–2328.

- (12) Wu, C.; Wang, J.; Chang, P.; Cheng, H.; Yu, Y.; Wu, Z.; Dong, D.; Zhao, F. Polyureas from Diamines and Carbon Dioxide: Synthesis, Structures and Properties. *Phys. Chem. Chem. Phys.* **2012**, *14*, 464–468.

- (13) Lu, X. B.; Ren, W. M.; Wu, G. P. CO<sub>2</sub> Copolymers from Epoxides: Catalyst Activity, Product Selectivity, and Stereochemistry Control. *Acc. Chem. Res.* **2012**, *45*, 1721–1735.

- (14) Darensbourg, D. J. Making Plastics from Carbon Dioxide: Salen Metal Complexes as Catalysts for The Production of Polycarbonates from Epoxides and CO<sub>2</sub>. *Chem. Rev.* **2007**, *107*, 2388–2410.

- (15) Kember, M. R.; Williams, C. K. Efficient Magnesium Catalysts for The Copolymerization of Epoxides and CO<sub>2</sub>; Using Water to Synthesize Polycarbonate Polyols. *J. Am. Chem. Soc.* **2012**, *134*, 15676–15679.

- (16) Coates, G. W.; Moore, D. R. Discrete Metal-based Catalysts for The Copolymerization of CO<sub>2</sub> and Epoxides: Discovery, Reactivity, Optimization, and Mechanism. *Angew. Chem., Int. Ed.* **2004**, *43*, 6618–6639.

- (17) Cheng, M.; Lobkovsky, E. B.; Coates, G. W. Catalytic Reactions Involving C1 Feedstocks: New High-activity Zn (II)-based Catalysts for the Alternating Copolymerization of Carbon Dioxide and Epoxides. *J. Am. Chem. Soc.* **1998**, *120*, 11018–11019.

- (18) Noh, E. K.; Na, S. J.; Sujith, S.; Kim, S.-W.; Lee, B. Y. Two Components in A Molecule: Highly Efficient and Thermally Robust Catalytic System for CO<sub>2</sub>/Epoxide Copolymerization. *J. Am. Chem. Soc.* **2007**, *129*, 8082–8083.

- (19) Ohkawara, T.; Suzuki, K.; Nakano, K.; Mori, S.; Nozaki, K. Facile Estimation of Catalytic Activity and Selectivities in Copolymerization of Propylene Oxide with Carbon Dioxide Mediated by Metal Complexes with Planar Tetradentate Ligand. *J. Am. Chem. Soc.* **2014**, *136*, 10728–10735.

- (20) Cohen, C. T.; Chu, T.; Coates, G. W. Cobalt Catalysts for the Alternating Copolymerization of Propylene Oxide and Carbon Dioxide: Combining High Activity and Selectivity. *J. Am. Chem. Soc.* **2005**, *127*, 10869–10878.

- (21) Luo, M.; Li, Y.; Zhang, Y. Y.; Zhang, X. H. Using Carbon Dioxide and Its Sulfur Analogues as Monomers in Polymer Synthesis. *Polymer* **2016**, *82*, 406–431.

- (22) Paddock, R. L.; Nguyen, S. T. Chemical CO<sub>2</sub> Fixation: Cr(III) Salen Complexes as Highly Efficient Catalysts for the Coupling of CO<sub>2</sub> and Epoxides. *J. Am. Chem. Soc.* **2001**, *123*, 11498–11499.

- (23) Zhuo, C.-W.; Qin, Y.-S.; Wang, X. H.; Wang, F. S. Steric Hindrance Ligand Strategy to Aluminum Porphyrin Catalyst for Completely Alternative Copolymerization of CO<sub>2</sub> and Propylene Oxide. *Chin. J. Polym. Sci.* **2018**, *36*, 252–260.
- (24) Wang, Y.; Qin, Y.; Wang, X. H.; Wang, F. S. Trivalent Titanium-salen Complex: Thermally Robust and Highly Active Catalyst for Copolymerization of CO<sub>2</sub> and Cyclohexene Oxide. *ACS Catal.* **2015**, *5*, 393–396.
- (25) Sugimoto, H.; Inoue, S. Copolymerization of Carbon Dioxide and Epoxide. *J. Polym. Sci., Part A: Polym. Chem.* **2004**, *42*, 5561–5573.
- (26) Byrne, C. M.; Allen, S. D.; Lobkovsky, E. B.; Coates, G. W. Alternating Copolymerization of Limonene Oxide and Carbon Dioxide. *J. Am. Chem. Soc.* **2004**, *126*, 11404–11405.
- (27) Cheng, M.; Moore, D. R.; Reczek, J. J.; Chamberlain, B. M.; Lobkovsky, E. B.; Coates, G. W. Single-Site  $\beta$ -DiiminateZinc Catalysts for the Alternating Copolymerization of CO<sub>2</sub> and Epoxides: Catalyst Synthesis and Unprecedented Polymerization Activity. *J. Am. Chem. Soc.* **2001**, *123*, 8738–8749.
- (28) Fukuoka, S.; Kawamura, M.; Komiya, K.; Tojo, M.; Hachiya, H.; Hasegawa, K.; Aminaka, M.; Okamoto, H.; Fukawa, I.; Konno, S. A Novel Non-Phosgene Polycarbonate Production Process Using By-Product CO<sub>2</sub> as Starting Material. *Green Chem.* **2003**, *5*, 497–507.
- (29) Song, B.; He, B.; Qin, A.; Tang, B. Z. Direct Polymerization of Carbon Dioxide, Dienes, and Alkyl Dihalides under Mild Reaction Conditions. *Macromolecules* **2018**, *51*, 42–48.
- (30) Yadav, N.; Seidi, F.; Crespy, D.; D'Elia, V. Polymers Based on Cyclic Carbonates as Trait d'Union Between Polymer Chemistry and Sustainable CO<sub>2</sub> Utilization. *ChemSusChem* **2019**, *12*, 724–754.
- (31) Guo, W.; Gómez, J. E.; Cristòfol, À.; Xie, J.; Kleij, A. W. Catalytic Transformations of Functionalized Cyclic Organic Carbonates. *Angew. Chem., Int. Ed.* **2018**, *57*, 13735–13747.
- (32) Hu, J.; Liu, H.; Han, B. Basic Ionic Liquids Promoted Chemical Transformation of CO<sub>2</sub> to Organic Carbonates. *Sci. China: Chem.* **2018**, *61*, 1486–1493.
- (33) Song, Q. W.; He, L. N. Robust Silver(I) Catalyst for the Carboxylative Cyclization of Propargylic Alcohols with Carbon Dioxide under Ambient Conditions. *Adv. Synth. Catal.* **2016**, *358*, 1251–1258.
- (34) Kimura, T.; Kamata, K.; Mizuno, N. A Bifunctional Tungstate Catalyst for Chemical Fixation of CO<sub>2</sub> at Atmospheric Pressure. *Angew. Chem., Int. Ed.* **2012**, *51*, 6700–6703.
- (35) Yoshida, Y.; Endo, T. Synthesis and Thermal Properties of Vinyl Copolymers with Phenyl Vinylethylene Carbonate and N-Substituted Maleimides Undergoing Color Change with Acid-base Switching. *Polym. Chem.* **2016**, *7*, 6770–6778.
- (36) Yoshida, Y.; Endo, T. Synthesis and Solid-state Properties of Crosslinked Alternating Copolymers of Phenyl Vinylethylene Carbonate and N-Substituted Maleimides. *J. Appl. Polym. Sci.* **2017**, *134*, 45247.
- (37) Yoshida, Y.; Endo, T. Radical Polymerization Behavior and Thermal Properties of Vinyl Ethylene Carbonate Derivatives Bearing Aromatic Moieties. *Polymer* **2016**, *102*, 167–175.
- (38) Miyaki, N.; Tomita, I.; Kido, J.; Endo, T. Synthesis of Novel Substituted Poly(arylene-vinylene)s by the Palladium-Catalyzed Three-Component Coupling Polymerization. *Macromolecules* **1997**, *30*, 4504–4506.
- (39) Choi, C. K.; Tomita, I.; Endo, T. Synthesis of Novel  $\pi$ -Conjugated Polymer Having An Enyne Unit by Palladium-Catalyzed Three-Component Coupling Polymerization and Subsequent Retro-Diels-Alder Reaction. *Macromolecules* **2000**, *33*, 1487–1488.
- (40) Sun, S.; Wang, B.; Gu, N.; Yu, J. T.; Cheng, J. Palladium-Catalyzed Arylcarboxylation of Propargylic Alcohols with CO<sub>2</sub> and Aryl Halides: Access to Functionalized  $\alpha$ -Alkylidene Cyclic Carbonates. *Org. Lett.* **2017**, *19*, 1088–1091.
- (41) Chen, L.; Lin, G.; Peng, H.; Ding, S.; Luo, W.; Hu, R.; Chen, S.; Huang, F.; Qin, A.; Zhao, Z.; Tang, B. Z. Sky-blue Nondoped OLEDs Based on New AIEgens: Ultrahigh Brightness, Remarkable Efficiency and Low Efficiency Roll-off. *Mater. Chem. Front.* **2017**, *1*, 176–180.
- (42) Zhang, H.; Zheng, X.; Kwok, R. T. K.; Wang, J.; Leung, N. L. C.; Shi, L.; Sun, J. Z.; Tang, Z.; Lam, J. W. Y.; Qin, A.; Tang, B. Z. In Situ Monitoring of Molecular Aggregation Using Circular Dichroism. *Nat. Commun.* **2018**, *9*, 4961.
- (43) Killops, K. L.; Campos, L. M.; Hawker, C. J. Robust, Efficient, and Orthogonal Synthesis of Dendrimers via Thiol-ene “Click” Chemistry. *J. Am. Chem. Soc.* **2008**, *130*, 5062–5064.
- (44) Hawker, C. J.; Frechet, J. M.; Grubbs, R. B.; Dao, J. Preparation of Hyperbranched and Star Polymers by A “Living”, Self-Condensing Free Radical Polymerization. *J. Am. Chem. Soc.* **1995**, *117*, 10763–10764.
- (45) Voit, B. I.; Lederer, A. Hyperbranched and Highly Branched Polymer Architectures Synthetic Strategies and Major Characterization Aspects. *Chem. Rev.* **2009**, *109*, 5924–5973.